

# CT Medical Images Denoising Based on New Wavelet Thresholding Compared with Curvelet and Contourlet

Amir Moslemi, Amir Movafeghi, Shahab Moradi

**Abstract**—One of the most important challenging factors in medical images is nominated as noise. Image denoising refers to the improvement of a digital medical image that has been infected by Additive White Gaussian Noise (AWGN). The digital medical image or video can be affected by different types of noises. They are impulse noise, Poisson noise and AWGN. Computed tomography (CT) images are subjects to low quality due to the noise. Quality of CT images is dependent on absorbed dose to patients directly in such a way that increase in absorbed radiation, consequently absorbed dose to patients (ADP), enhances the CT images quality. In this manner, noise reduction techniques on purpose of images quality enhancement exposing no excess radiation to patients is one the challenging problems for CT images processing. In this work, noise reduction in CT images was performed using two different directional 2 dimensional (2D) transformations; i.e., Curvelet and Contourlet and Discrete Wavelet Transform (DWT) thresholding methods of BayesShrink and AdaptShrink, compared to each other and we proposed a new threshold in wavelet domain for not only noise reduction but also edge retaining, consequently the proposed method retains the modified coefficients significantly that result good visual quality. Data evaluations were accomplished by using two criterions; namely, peak signal to noise ratio (PSNR) and Structure similarity (Ssim).

**Keywords**—Computed Tomography (CT), noise reduction, curve-let, contour-let, Signal to Noise Peak-Peak Ratio (PSNR), Structure Similarity (Ssim), Absorbed Dose to Patient (ADP).

## I. INTRODUCTION

COMPUTED TOMOGRAPHY (CT) images are basically acquired by analytical signal processing of attenuated radiation exposed to the body. Initially, originating in radiation source, beam line diversion, radiation attenuation in the body, backscattering radiation, detectors sensitivity up to images reconstruction, there are many factors each of which affecting accumulative noise.

Absorbed radiation in detectors is the most important noise factor amongst all for CT images. The higher exposure the detectors receive, the higher signal to noise ratio (SNR) in the acquired CT images subsequently higher images quality is achieved. However, absorbed dose to patients (ADP) will be increased as well which makes a limitation for acquisition high quality images. Since the 90s decade, CT scan systems have been developing enormously worldwide continuously. Thus, monitoring the ADP for the patients taking CT images

Amir Moslemi is with the Department of Energy Engineering, Sharif University of Technology, P.O. Box 11365-8639, Tehran, Iran (phone: 00989394342249, e-mail: moslemi@energy.sharif.ir).

Amir Movafeghi is with the Nuclear Safety and Radiation Protection Research Group, Nuclear Sciences and Technologies Research Center, AEOI (e-mail: amovafeghi@aeoi.org.ir).

has been also investigated more seriously by researcher. There have been numerous surveys on patient dose in CT in different countries and regions and with varying focus with respect to CT applications and anatomic ranges. A good general overview on long-term developments has been provided by UNSCEAR (Table I) [1].

Regarding this fact, ADP reduction in CT images has been performed via many different methods not only to guarantee safety issues but also to maintain high quality of CT images. Most of these methods are based on the hardware developments such as detectors efficiency enhancement and phased array detectors utilization while there are others with software manipulation including image reconstruction (IR) or Fourier back projection (FBP). In practice, noise reduction by manipulating radiation exposure could be executed by voltage, current or exposure time increase all of them result in ADP increase. Image processing techniques and software approach in general with lower prices than hardware solutions are able to provide high quality images with no more radiation exposure. In this work, noise reduction and quality enhancement of CT images were achieved by using 2D Curvelet and Contourlet transformations in comparison with Wavelet thresholding method.

TABLE I  
TRENDS IN AVERAGE DOSES PER CT EXAMINATION IN COUNTRIES OF HEALTH CARE LEVEL I [1]

| Expected Interval | Average Equivalent Dose (sv) |
|-------------------|------------------------------|
| 1976-179          | 1.3                          |
| 1980-1991         | 4.4                          |
| 1991-1196         | 8.8                          |
| 1996-2007         | 7.4                          |

Sv is unit of dose.

The contourlet and curvelet transforms were developed over several years in an attempt to break an inherent limit plaguing wavelet denoising of images. This limit arises from the well-known and frequently depicted fact that the two-dimensional (2-D) wavelet transform of images exhibits large wavelet coefficients even at fine scales, all along the important edges in the image, so that in a map of the large wavelet coefficients one sees the edges of the images repeated at scale after scale. While this effect is visually interesting, it means that many wavelet coefficients are required in order to reconstruct properly the edges of the image. Denoising faces certain difficulties due to estimate of coefficients. There is, owing to well-known statistical principles, an imposing tradeoff between parsimony and accuracy which even in the best balancing leads to a relatively high mean squared error (MSE).

In the recent years, there has been a fair amount of research

on thresholding and threshold selection procedures for image denoising. The threshold selection plays an important role in image denoising because the large value of the threshold kills the image data, while the small value of threshold keeps the noisy data.

## II. MATERIALS AND METHODS

### A. CT Images Acquisition

CT images were acquired from Noor Eye Hospital and clinics in Iran, we analysed CT images.

### B. Curvelet Transform for Image Denoising

Curvelet transformation method is based on multiple scale Ridgelet transform method. Curvelet transform coefficients are derived by operation of single scale Ridgelet transformation on different sub-bands frequency domains in Wavelet transform. The detail steps of Curvelet transformation are described as below.

Supposing 2D function  $f(x_1, x_2)$ , if filter  $\Delta_s$  supplies a band in  $f(x_1, x_2)$  domain in neighborhood  $|\varepsilon| \in [2^{2s}, 2^{2s+2}]$  and if  $P$  is a low-pass filter for band  $|\varepsilon| \leq 1$ ;  $f(x_1, x_2)$  will be divided in the following subband frequency domains described below shown schematically in Fig. 1.

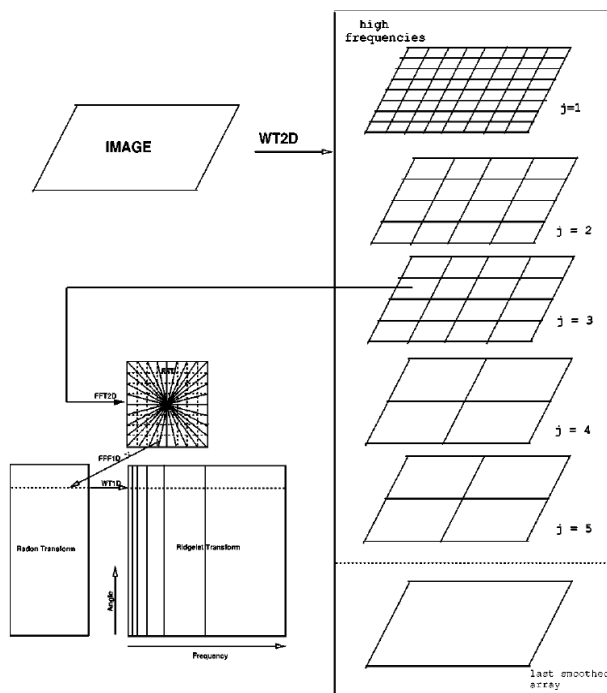


Fig. 1 Curvelet transform steps for sectioning the image to different sub-band frequency domains [4]

- Sectioning the Image to different subband frequency domains in Wavelet transform
- Distinguishing each frequency domain into desirable scale squares by uniform masks
- Normalization of the squares
- Operating Ridgelet transformation on each normalized

square

Fine edges of the image could be sharply defined by local Ridgelet transform because of the fact that curves resemble straight lines in fine scales [4].

A novel technique of noise reduction by Curvelet method is proposed by Donoho and Stack. In this technique, domains are thresholding as below:

$$\hat{x}_i = \begin{cases} y_i & |y_i| \geq \lambda \\ 0 & |y_i| < \lambda \end{cases} \quad (1)$$

$$\lambda = k \cdot \hat{\sigma}_i \cdot \sigma \quad (2)$$

where  $\lambda$ ,  $\sigma^2$  is thresholding level and noise variance, respectively. Unlike Wavelet transformation, it is not an isometric transform. So, variance for each  $\hat{\sigma}_i$  was estimated by Monte Carlo simulation. For this purpose, several noisy images were simulated by coding in Monte Carlo method.

Regarding Stack's proposal  $k$  was chosen 4 and 3 respectively for single and multi-scale transform.

### C. Contourlet Transform for Image Denoising

Contourlet transform is a directional 2D transformation proper for displaying images, curves, contours, etc. with fine structures in detail. This transformation not only inherits the Wavelet transform properties such as localization of space-frequency and multi-distinguishable display but also possesses other properties such as being directional and anisotropic. It is consisted of Laplacian Pyramid and directional filters bank. Laplacian Pyramid is used for obtaining discrete points and the directional filters bank is utilized for connecting discrete points to linear structure. Laplacian Pyramid structure is shown in Fig. 2.

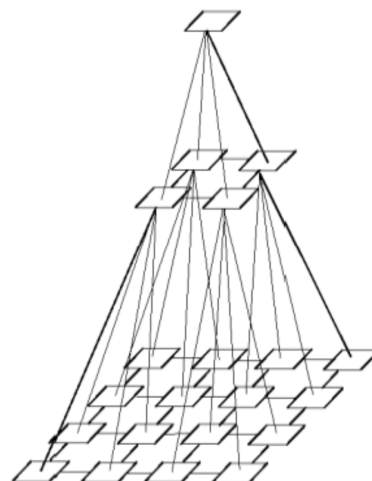


Fig. 2 Laplacian Pyramid structure [5]

To operate the Curvelet transformation, a pseudo Wavelet transformation on purpose of edge sharpening followed by another local directional transformation is utilized on the

image to discern the contour details. Finally, Contourlet, the expansion of the image on basis of Contour detail elements is achieved.

Contourlet is invariant to scales and directions. Therefore, soft contour will be estimated by Contourlet transform in some few distinguishing steps shown in Fig. 3. In this manner, Contourlet transform in frequency domain supplies directional multi scale decomposition.

Laplacian Pyramid is one the methods for multi scale decomposition of image. Bamberger and Smith have established a 2D filters bank suitable for optimized reconstruction with maximum frequency elimination. As a matter of fact, filters bank decomposing an  $l$  level binary tree yields  $2^l$  subband with triangle frequency domain as shown in Fig. 4.

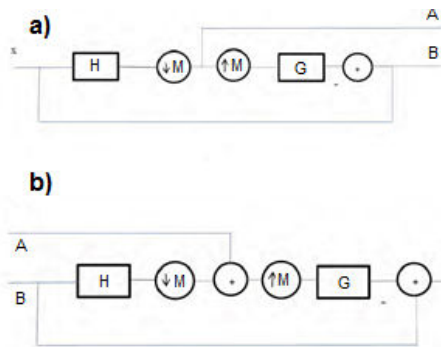


Fig. 3 Laplacian Pyramid structure. a) a schematic of one level decomposition and b) diagram of new structure for Laplacian pyramid. A, B, G, H, and M denote, low-pass filter, high-pass filter and sampling matrix [5]

Filters bank is designated for manipulating high frequencies of input images containing directional information. It infrequently operates on low frequency bands. To better understand frequency domains Fig. 5 displays multi scale frequency decomposition, low frequencies are also allowed in some directional subbands. Hereto, directional filters bank is not able to provide scarce display of the images. Therefore, combining directional filters bank with Laplacian Pyramid makes the Contourlet filters bank suitable for decomposing images to multi scale directional subbands.

Initially, images are induced by Laplacian Pyramid followed by operation of directional filters bank. Thus, directional information is derived in such manner. The same steps will be repeated for the low-frequency domains of the image by low-pass filters.

Contourlet has special properties one of which is its definition expansion on quadrangle nets. Taking such property in account, interpretation and manipulation of image pixels are fulfilled in uniform discrete quadrangle nets. This is related to the fact that in such geometry there are much more central frequency squares rather than polar geometry [5], [6].

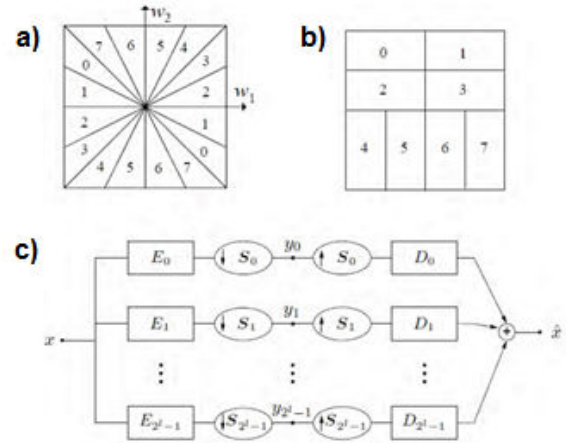


Fig. 4 Frequency sectioning for filters bank with 8 bands a) frequency domains for 3 levels and 8 bands triangle frequency domains, b) sub-bands 0 to 3 relate to horizontal directions while subbands 4 to 7 relate to vertical directions, and c) afore mentioned steps for operating filters on Fig. 3 [5]

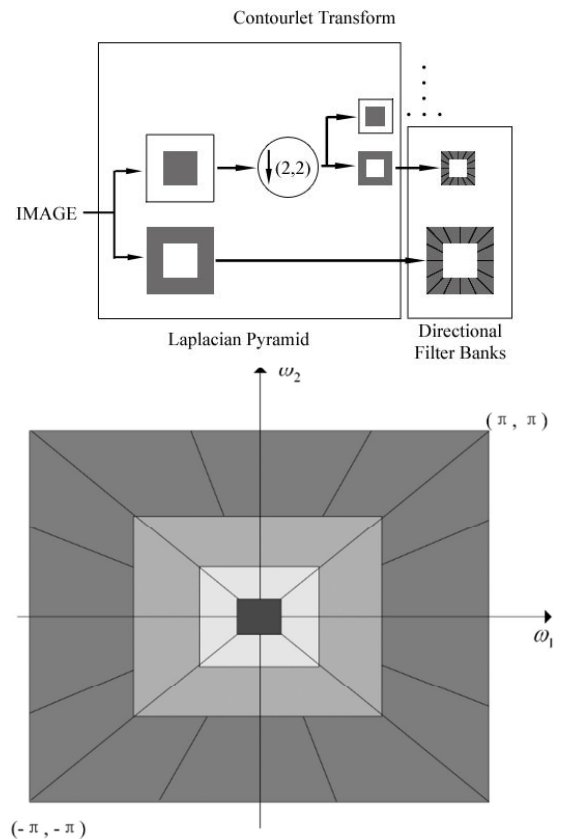


Fig. 5 Contourlet filters bank. Multi scale decomposition obtained from Laplacian Pyramid operated on octet bands. Then, directional filters banks operated on the channels

### III. 2D WAVELET TRANSFORM FOR IMAGE DE-NOISING

2D Wavelet transform divides images to 4 sub-images  $I_a$ ,  $I_D$ ,  $I_H$  and  $I_V$ . Sub-images  $I_D$ ,  $I_H$  and  $I_V$  denote diagonal, horizontal and vertical directions of the main image respectively. In other words,  $I_H$  illustrates the horizontal edge

of the image (vertical frequency) while  $I_V$  denotes the vertical edge of the image (horizontal frequency). Regarding filters concept as shown in Figs. 6 and 7, sub-image  $I_a$  has been influenced by two low pass filters (Low-Low). As for the sub-images  $I_D$ ,  $I_H$  and  $I_V$ , there would be High-High, High-Low and Low-High filters respectively [2]-[12].

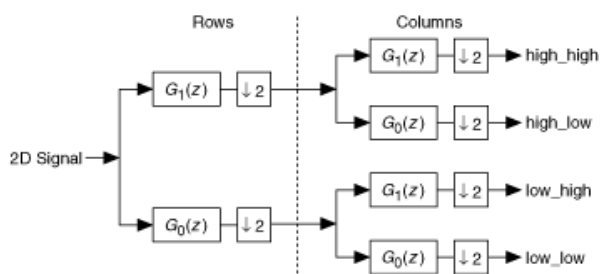


Fig. 6 Discrete Wavelet filters bank

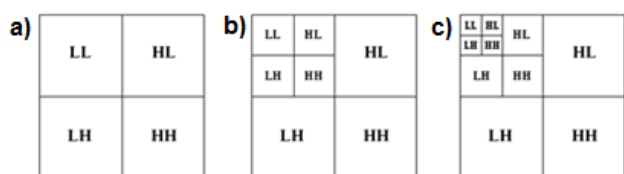


Fig. 7 Frequency level sectioning: a) the first level of sectioning, b) two dimensional wavelet transform and c) the third level of sectioning

#### IV. IMAGE DE-NOISING BY WAVELET THRESHOLDING

##### A. BayesShrink Threshold

Thresholding in Wavelet transform is one the most conventional methods for noise reduction. Thresholds are divided to soft and hard categories. The soft threshold is continuous so is used for smoothing the image. On the other side, hard threshold is discontinuous, so it's applied for edge sharpening similar to Gibbs's effect. There are three main thresholding methods; namely, VisueShrink, SureShrink and BayesShrink. BayesShrink method proposed by Chang is potential for improvement image quality 8% and 5% higher than SureShrink and VisueShrink methods respectively. In this work, BayesShrink method was applied for noise reduction due to the higher SNR and lower standard deviations rather than two other methods. One of the most popular methods namely, BayesShrink was proposed by Chang et al. in which the threshold was derived from Bayesian method [5], [6]. This method has better performance than the SureShrink in terms of mean square error (MSE) [3], [7], [8], [10]. The BayesShrink threshold for every sub-bands is given as follows:

$$T_{Bayes} = \frac{\sigma^2}{\sigma_Y} \quad (3)$$

where,  $\sigma_Y$  is additive Gaussian noise and  $\sigma$  is the noise variance that is define as:

$$\sigma^2 = [\text{median}(|Y_i, j|)/0.6745]^2 \quad (4)$$

##### B. Adaptshrink

Chang et al. generalized BayesShrink method so as to achieve a comparative spatial thresholding method. In this method, each of sub-band coefficients are modeled separately as GGD random numbers on contrary of conventional method in which all coefficients are modeled as one GGD random variable. To investigate more, suppose a noisy image with sub-band  $S$  containing  $M^2$  coefficients ( $Y_{ij}, i, j = 1, \dots, M$ ). There is a neighborhood with absolute value of weighted average ( $Z_{ij}$ ) for each coefficients ( $Y_{ij}$ ). If the neighborhood of some desirable coefficient ( $Y_{i_0, j_0}$ ) has  $2l + 1$  coefficients called as set  $B_{i_0, j_0}$ , variance is defined as [9]:

$$\hat{\sigma}_x^2[i_0, j_0] = \max \left\{ \left( \frac{1}{2l + 1} \sum_{[k, l] \in B_{i_0, j_0}} Y_{k, l}^2 \right) - \sigma^2, 0 \right\} \quad (5)$$

Calculating variances for all coefficients, thresholding level is obtained from:

$$\lambda_s[i_0, j_0] = \frac{\hat{\sigma}^2}{\hat{\sigma}_x[i_0, j_0]} \quad (6)$$

#### V. PROPOSED NEW THRESHOLD FOR IMAGE DE-NOISING

The Threshold function that can retain edges must be similar to hard threshold. In this paper we proposed semi-hard threshold for noise removing and edge preservation [11], therefore,  $\psi_\alpha$  is the threshold function that is defined as:

$$\psi_\alpha(x, \lambda) = \begin{cases} \varepsilon \left( \frac{e^{\alpha|x|} - 1}{n} \right) \cdot \text{sgn}(x), & |x| \leq \lambda \\ \left( \frac{|x| + ke^{-\alpha|x|}}{n} \right) \cdot \text{sgn}(x), & |x| > \lambda \end{cases} \quad (7)$$

$$\varepsilon = \frac{(\lambda\alpha + 1)e^{-\lambda\alpha}}{\alpha(2 - e^{-\lambda\alpha})} \quad (8)$$

$$k = \frac{(1 - \lambda\alpha)e^{\lambda\alpha} - 1}{\alpha(2 - e^{-\lambda\alpha})} \quad (9)$$

where, level of threshold be determind by  $\alpha$  parameter and  $n$  is any positive integer i.e.  $n > 0$ . This thresholding function tends to hard threshold by increase  $\alpha$ . The two other threshold parameter  $\varepsilon$  and  $k$  determine so that the function and derivative function is continuous. This threshold function inspired by soft and hard threshold. The decomposition level has been used "sym4" wavelet because "sym4" wavelet is symmetry.

#### VI. RESULT AND DISCUSSION

Evaluation of images quality was accomplished by calculating PSNR and Ssim as (7) and (9) respectively. The acquired data are presented in Tables II and III.

$$PSNR = 10 \log_{10} \frac{(\max I)^2}{MSE} \quad (10)$$

in which  $MSE$  is defined as:

$$MSE = \frac{1}{m \times n} \sum_{i=0}^{m-1} \sum_{j=0}^{n-1} [I(i, j) - K(i, j)]^2 \quad (11)$$

where  $m \times n$ ,  $I(i, j)$  and  $K(i, j)$  stand for image size, original image and de-noised image, respectively.

$$S_{sim} = \frac{(2\mu_x \mu_y)(2\sigma_{xy} + C_2)}{(\mu_x^2 + \mu_y^2 + C_1)(\sigma_x^2 + \sigma_y^2 + C_2)} \quad (12)$$

in which  $\mu_x$ ,  $\mu_y$ ,  $\sigma_x$ ,  $\sigma_y$  and  $\sigma_{xy}$  are mean value of image  $x$ , mean value of image  $y$ , standard deviation of image  $x$ , standard deviation of image  $y$  and covariance of the  $x, y$  respectively.  $C_1 = (k_1 L_1)^2$  and  $C_2 = (k_2 L_2)^2$  where  $L$  is the variation range.  $k_1 = 0.01$  and  $k_2 = 0.03$  were proposed by Wang et al. SSIM considers image degradation as perceived change in structural information. Structural information is the idea that the pixels have strong inter-dependencies especially when they are spatially close.

TABLE II  
 PSNR RESULT FOR MEDICAL CT IMAGES

| Noise Reduction Method | Type of Images | Noise Level 10 | Noise Level 30 | Noise level 50 |
|------------------------|----------------|----------------|----------------|----------------|
| Curvelet               | Image a        | 33/07          | 26/95          | 25/73          |
|                        | Image b        | 32/77          | 26/35          | 25/34          |
|                        | Image c        | 32/63          | 26/17          | 25/21          |
| Contourlet             | Image a        | 33/13          | 27/07          | 25/83          |
|                        | Image b        | 33/01          | 26/77          | 25/43          |
|                        | Image c        | 32/89          | 26/43          | 25/37          |
| AdaptShrink            | Image a        | 32/43          | 26/06          | 23/83          |
|                        | Image b        | 32/27          | 25/91          | 23/58          |
|                        | Image c        | 32/12          | 25/79          | 23/21          |
| BayesShrink            | Image a        | 31/17          | 25/13          | 22/83          |
|                        | Image b        | 31/03          | 24/98          | 22/51          |
|                        | Image c        | 30/97          | 24/76          | 22/31          |
| Proposed method        | Image a        | 33/11          | 27/01          | 25/81          |
|                        | Image b        | 32/86          | 26/59          | 25/39          |
|                        | Image c        | 32/71          | 26/27          | 25/19          |

Different noise variances were added to the images. However, in this work, variances 10, 30 and 50 were reported.

Regarding *PSNR* criterion in the images, it is obvious that proposed method revealed better noise reduction rather than Curvelet and Contourlet transform, Adapt Shrink and Bayes Shrink thresholding.

The other worth mentioning domination of Curvelet and Contourlet transform against Wavelet transform thresholding was the image information maintenance especially at the sharp edges after the transformation operation acquired by Ssim criterion; therefore, we can see the better result for retain edge and image details by proposed method rather than AdaptShrink and BayesShrink.

Noise reduction in CT images results in images quality enhancement at the same expected level of ADP. However, raising the precession of measurements is subject to utilization of PMMA (dose measurement phantom) phantoms. Such phantoms are exposed at both high and low dose radiation. Subsequently, the image processing algorithm will be operated on the acquired low dose images to evaluate the noise

reduction, hence quality enhancement compared to high dose image with no image processing manipulation.

TABLE III  
 SSIM RESULT FOR MEDICAL CT IMAGES

| Noise Reduction Method | Type of Images | Noise Level 10 | Noise Level 30 | Noise level 50 |
|------------------------|----------------|----------------|----------------|----------------|
| Curvelet               | Image a        | 0.9896         | 0.883          | 0.603          |
|                        | Image b        | 0.9771         | 0.881          | 0.598          |
|                        | Image c        | 0.9713         | 0.879          | 0.591          |
| Contourlet             | Image a        | 0.9895         | 0.8856         | 0.612          |
|                        | Image b        | 0.9863         | 0.8813         | 0.601          |
|                        | Image c        | 0.9817         | 0.8801         | 0.593          |
| AdaptShrink            | Image a        | 0.976          | 0.727          | 0.432          |
|                        | Image b        | 0.971          | 0.719          | 0.428          |
|                        | Image c        | 0.965          | 0.721          | 0.417          |
| BayesShrink            | Image a        | 0.974          | 0.713          | 0.42           |
|                        | Image b        | 0.971          | 0.709          | 0.418          |
|                        | Image c        | 0.967          | 0.703          | 0.412          |
| Proposed method        | Image a        | 0.9832         | 0.8801         | 0.596          |
|                        | Image b        | 0.9814         | 0.794          | 0.588          |
|                        | Image c        | 0.9801         | 0.789          | 0.581          |



Image (a) Image (b) Image (c)

Fig. 8 Medical CT images that used for processing

## VII. CONCLUSION

CT dose reduction is of great interest but very challenging. Acquired sequences involved higher levels of noise, very low contrast, and require preserving high frequency content, which makes common de-noising methods fail. We presented an original method based on a Thresholding in the Wavelet domain. Peak signal to noise ratio (PSNR) calculation in CT images revealed that proposed method algorithms applied in this work diminish noise much better than Curvelet and Contourlet transform and AdaptShrink and BayesShrink thresholding. Ssim criterion comparison in both techniques illustrated that Curvelet and Contourlet transform not only maintain the images information invariant but also intensify the edges vividness. In sum, proposed method, Curvelet and Contourlet transform with all such worthy advantages are promising for images quality enhancement in the medical images processing field and clinical applications.



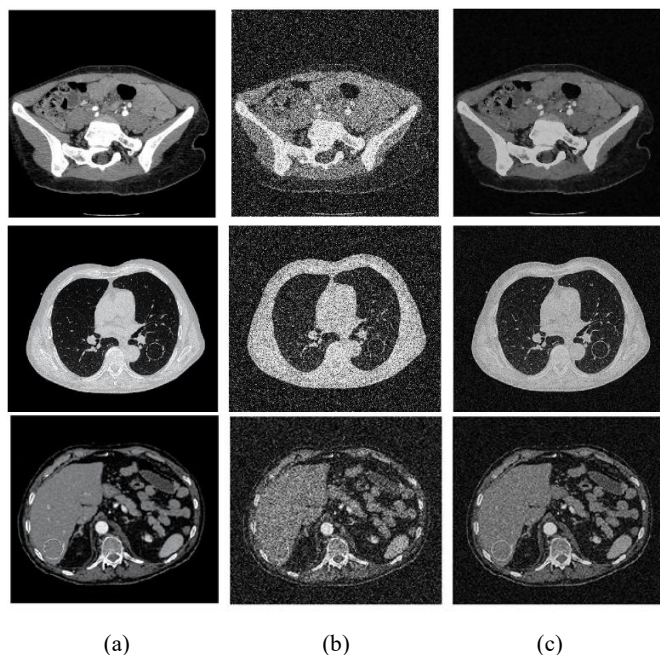


Fig. 9 (a) Original image (b) Noisy image (c) Image de-noised by proposed method

#### REFERENCES

- [1] Willi A. Kalender, "Dose in x-ray computed tomography", *Physics in Medicine and Biology*, Phys. Med. Biol. 59 (2014) R129–R150.
- [2] Gonzalez. R. C and. Wood R.E, "Digital Image Processing", 2<sup>nd</sup> edition, New Jersey Prentice Hall, 2002.
- [3] R. R. Coifman and A. Sowa, "Combining the calculus of variations and wavelets for image enhancement," *Appl. Comput. Harmon. Anal.*, vol. 9, no. 1, pp. 1–18, Jul. 2000.
- [4] Jean-Luc Starck, Emmanuel J. Candès, and David L. Donoho, "The Curvelet Transform for Image Denoising". *IEEE Transactions on Image Processing*, Vol. 11, No. 6, June 2002.
- [5] Minh N Do and Martin Vetterli, Fellow, IEEE, "The Contourlet Transform: An Efficient Directional Multiresolution Image Representation", *IEEE Transaction On Image Processing*, December 2005.
- [6] Shao-Weidal, Yan-Kuisun, Xiao-Lin Tian, Ze-Sheng Tang, "Image Denoising Based On Complex Contourlet Transform", *International Conference on Wavelet Analysis and Pattern Recognition*, Beijing, China, 2-4 Nov .2007.
- [7] J. Hou , J. Tian, and J. Liu, "An improved Wienerchop algorithm for image denoising", in *Proc. of the IEEE International Conference on Communications, Circuits and Systems (ICCCAS)*, vol. 2, pp. 838–841, Oct. 2005.
- [8] S. G. Chang, B. Yu, and M. Vetterli, "Spatially adaptive wavelet thresholding with context modeling for image denoising," *IEEE Trans. Image Process.*, vol. 9, no. 9, pp. 1522–1531, 2000.
- [9] S. G. Chang, B. Yu, and M. Vetterli, "Adaptive wavelet thresholding for image denoising and compression," *IEEE Trans. Image Processing*, vol. 9, no. 9, pp. 1532–1546, 2000.
- [10] R. R. Coifman and A. Sowa, "Combining the calculus of variations and wavelets for image enhancement," *Appl. Comput. Harmon. Anal.*, vol. 9, no. 1, pp. 1–18, Jul. 2000.
- [11] Mantosh Biswas and Hari Om, "An Image Denoising Threshold Estimation Method" *Advances in Computer Science and its Applications (ACSA)* 377 Vol. 2, No. 3, 2013, ISSN 2166-2924.
- [12] A. K. Velmurugan and Dr. R. Jagadeesh Kannan, "Wavelet Analysis For Medical Image Denoising Based on Thresholding Technique", *International conference on current Trends in Engineering and Technology, ICCTET'13*, pp.213-215,2013.